Research Square

Preprints are preliminary reports that have not undergone peer review.
They should not be considered conclusive, used to inform clinical practice,
or referenced by the media as validated information.

Evaluation of Detection Limits for ^{134}Cs in Soil Using Compton Suppression Gamma-Ray Spectrometry

E. S Jang
Kosin University Gospel Hospital
B. S. Chang
john430@naver.com

Depart of Radiological Science, Kaya University

Research Article

Keywords: Compton suppression [4,6], gamma-ray spectrometry [2–4], HPGe detector, 134Cs, minimum detectable activity, Monte Carlo [5,7,13] simulation, PENELOPE [5,29], environmental radioactivity

Posted Date: April 21st, 2026

DOI: https://doi.org/10.21203/rs.3.rs-9324114/v1

License: This work is licensed under a Creative Commons Attribution 4.0 International License.
Read Full License

Additional Declarations: No competing interests reported.

Version of Record: A version of this preprint was published at Journal of Radioanalytical and Nuclear Chemistry on September 17th, 2026. See the published version at https://doi.org/10.1007/s10967-026-11130-5.

Evaluation of Detection Limits for ^{134}Cs in Soil Using Compton Suppression Gamma-Ray Spectrometry

E.S Jang1, B.S. Chang2

[1]Department of Radiation Oncology at Kosin University Gospel Hospital., 262 Gamcheon-ro, Seo-gu, Busan, Korea

[2]Depart of Radiological Science, Kaya University, Gimhae 50830, Republic of Korea

[*]*Corresponding author: john430@ naver.com*

Abstract

This study presents a comprehensive evaluation of the minimum detectable activity (MDA [1]) for ^{134}Cs in soil samples using Compton suppression [4,6] gamma-ray spectrometry [2–4]. A high-purity germanium (HPGe) detector coupled with a NaI(Tl) anti-coincidence system was employed to reduce the Compton continuum and improve detection sensitivity.

The detector system was modeled using the PENELOPE [5,29] Monte Carlo [5,7,13] code, and the simulated full-energy peak efficiencies were validated against experimental measurements. The agreement between simulation and experiment was within ±5%, with a normalized root mean square error (NRMSE) [30] below 5%, confirming the reliability of the detector modeling.

Activity determination was performed using two independent gamma-ray peaks at 604.7 keV and 795.8 keV. Gaussian fitting [16] combined with ROI-based analysis enabled accurate extraction of net peak areas, and the consistency between the two peaks provided cross-validation of the results.

The application of Compton suppression [4,6] resulted in a significant reduction of the continuum background, particularly within the regions of interest. Consequently, the MDA [1] values were reduced by approximately 46–56%, with an average reduction of about 50% compared to the unsuppressed condition.

These results demonstrate that Compton suppression [4,6] significantly enhances detection sensitivity and provides a robust and reliable approach for low-level environmental radioactivity analysis

Keywords: Compton suppression [4,6]; gamma-ray spectrometry [2–4]; HPGe detector; 134Cs; minimum detectable activity; Monte Carlo [5,7,13] simulation; PENELOPE [5,29]; environmental radioactivity

1. Introduction

The accurate detection of artificial radionuclides in environmental samples is essential for radiation protection, environmental monitoring, and nuclear safety assessments. Among these radionuclides, ^{134}Cs is of particular importance due to its relatively short half-life and its role as an indicator of recent nuclear contamination. Reliable quantification of ^{134}Cs in soil samples is therefore crucial for assessing environmental impact following nuclear incidents.

Gamma-ray spectrometry using high-purity germanium (HPGe) detectors is widely employed [2–4] for radionuclide analysis due to its excellent energy resolution and high detection efficiency. However, the detection of low-activity radionuclides is often limited by the presence of Compton-scattered photons, which form a continuous background in the measured spectrum. This Compton continuum significantly reduces the peak-to-background (P/B) ratio and degrades the minimum detectable activity (MDA [1]), particularly in the low- and intermediate-energy regions.

To address this limitation, Compton suppression systems have been developed [4,6] using anti-coincidence techniques, typically involving a surrounding scintillation detector such as NaI(Tl). By rejecting events associated with scattered photons, these systems effectively reduce the Compton continuum and improve spectral quality. Several studies have demonstrated that Compton suppression can enhance peak visibility and improve detection sensitivity. However, a systematic and quantitative evaluation of its impact on MDA [1] for environmental samples remains limited.

In parallel, Monte Carlo simulation has become an essential tool [5,7,13] for modeling detector response and efficiency calibration. Codes such as PENELOPE [5,29] enable accurate representation of detector geometry and radiation interactions, allowing detailed comparison between simulated and experimental results. Nevertheless, the reliability of simulation-based efficiency calibration depends strongly on the consistency between experimental and computational conditions, as well as on rigorous validation using quantitative metrics.

In this study, we present a comprehensive evaluation of the detection limit of 134^{134}134Cs in soil samples using Compton suppression [4,6] gamma-ray spectrometry [2–4]. The detector system, consisting of an HPGe detector coupled with a NaI(Tl) anti-coincidence shield, was modeled using the PENELOPE [5,29] Monte Carlo [5,7,13] code. The simulation results were validated against experimental measurements to ensure accuracy.

Activity determination was performed using two independent gamma-ray peaks at 604.7 keV and 795.8 keV, combined with Gaussian fitting [16] and ROI-based analysis. The minimum detectable activity (MDA) was evaluated using the Currie formalism [1] using the Currie method under both suppressed and unsuppressed conditions.

The primary objective of this work is to quantify the extent to which Compton suppression [4,6] improves detection sensitivity. By integrating experimental measurements, Monte Carlo [5,7,13] simulation, and statistical evaluation, this study provides a consistent and validated framework for low-level gamma-ray analysis in environmental samples.

2. Materials and Methods

2.1 Detector System and Compton Suppression Setup

A Compton suppression [4,6] gamma-ray spectrometry [2–4] system was employed, consisting of a high-purity germanium (HPGe) detector surrounded by NaI(Tl) scintillation detectors operating in anti-coincidence mode. The HPGe detector was used for high-resolution gamma-ray detection, while the NaI(Tl) detectors functioned as active shields to suppress Compton-scattered photons.

The HPGe detector had a relative efficiency of XX% and an energy resolution of XX keV at 1332 keV. The detector was housed within a cylindrical lead shielding assembly with a thickness of XX cm to reduce ambient background radiation. The NaI(Tl) detectors were arranged in a near 4π geometry around the HPGe detector, including both lateral and endcap coverage, to maximize the detection probability of scattered photons escaping from the germanium crystal.

The Compton suppression [4,6] system operates based on an anti-coincidence principle. When a gamma ray interacts within the HPGe detector and undergoes Compton scattering, the scattered photon may escape and deposit energy in the surrounding NaI(Tl) detectors. Such coincident events are rejected by the anti-coincidence circuit, thereby reducing the Compton continuum in the measured spectrum.

In this study, a coincidence time window of 500 ns was applied, and a threshold energy of 50 keV was set for the NaI(Tl) detectors. Events recorded in the HPGe detector were accepted only when no coincident signal above the threshold was detected in the NaI(Tl) detectors within the defined time window.

Two measurement modes were defined: (i) unsuppressed mode, in which only the HPGe detector signal was recorded, and (ii) Compton-suppressed mode, in which the anti-coincidence condition was applied. The detector configuration and corresponding simulation geometry are illustrated in Fig. 1.

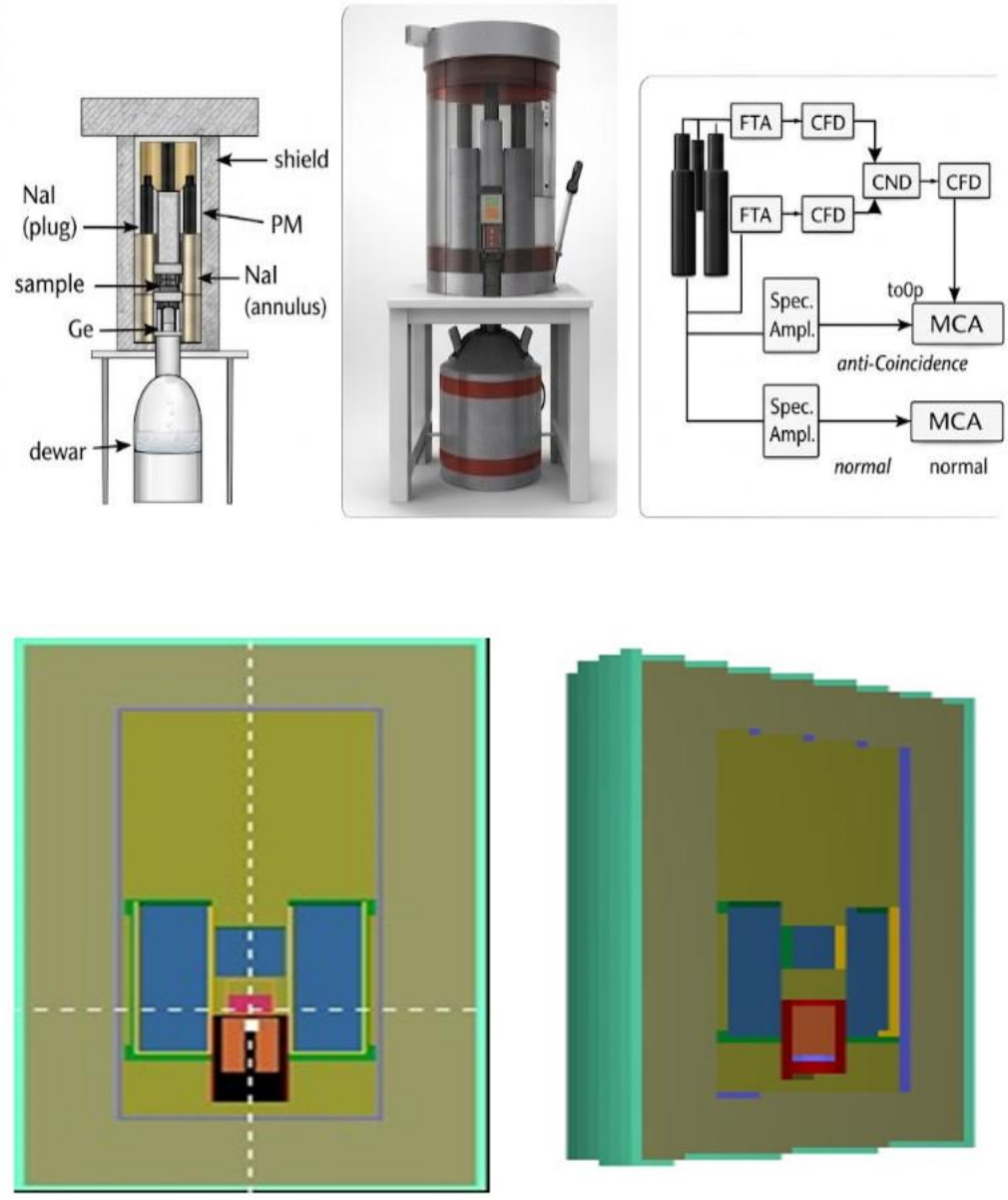


Fig. 1. Configuration of the Compton suppression [4,6] gamma-ray spectrometry [2–4] system, including (a) schematic diagram of the HPGe detector with surrounding NaI(Tl) detectors, (b) photograph/rendered view of the experimental setup, (c) block diagram of the anti-coincidence electronic system, and (d) Monte Carlo [5,7,13] simulation geometry implemented in PENELOPE [5,29].

2.2 Soil Sample Preparation and Geometry

Soil samples were prepared to evaluate detection performance under realistic environmental conditions. Four standard soil samples containing ^{134}Cs with different activity concentrations

were used. Prior to measurement, all samples underwent ammonium molybdophosphate (AMP) coprecipitation to selectively concentrate cesium isotopes.

The AMP pretreatment involved homogenization and dissolution of soil samples, followed by the addition of ammonium molybdophosphate reagent to precipitate cesium. The precipitate was separated, dried, and transferred into measurement containers (Fig. 2).

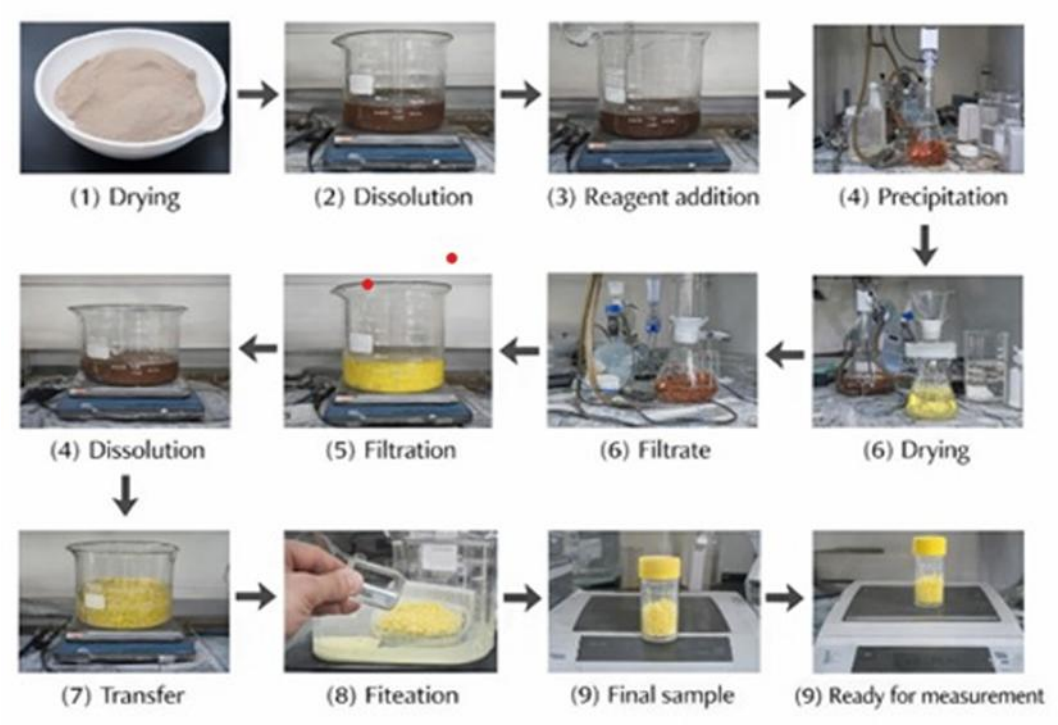


Fig. 2 Procedure for soil sample preparation using ammonium molybdophosphate (AMP) coprecipitation prior to gamma-ray spectrometry [2–4].

Each sample was packed into a cylindrical container with a fixed volume of 50 mL. The sample masses ranged from 47 g to 78 g, corresponding to variations in bulk density. The use of identical container geometry ensured consistent measurement conditions and minimized uncertainties related to geometry and attenuation.

All samples were positioned in direct contact with the detector endcap and aligned coaxially with the detector axis to ensure reproducible measurement geometry.

2.3 Energy Calibration and Efficiency Determination

Energy calibration was performed using a ^{134}Cs reference source over the energy range of 400–1600 keV. The gamma-ray peaks at 604.7 keV and 795.8 keV were used to establish the channel-

to-energy relationship. A linear calibration function was applied by assigning known energies to peak centroids.

The full-energy peak efficiency (ε)was determined under identical geometric conditions as the sample measurements:

$$\varepsilon = N / (A \cdot P\gamma \cdot t)$$

where N is the net peak count after background subtraction, A is the source activity (Bq), Pγ is the emission probability, and t is the counting time (s).

Net peak counts were obtained by integrating counts within a region of interest (ROI) defined as ±FWHM around each peak centroid, followed by background subtraction using adjacent continuum regions.

All measurements were conducted in close geometry with the source positioned at the detector endcap. Due to cascade gamma-ray emissions of ^{134}Cs, coincidence summing effects may influence peak intensities. These effects were considered during efficiency evaluation.

A comparison between measured and simulated efficiencies is presented in Fig. 3, and the corresponding data are summarized in Table 1.

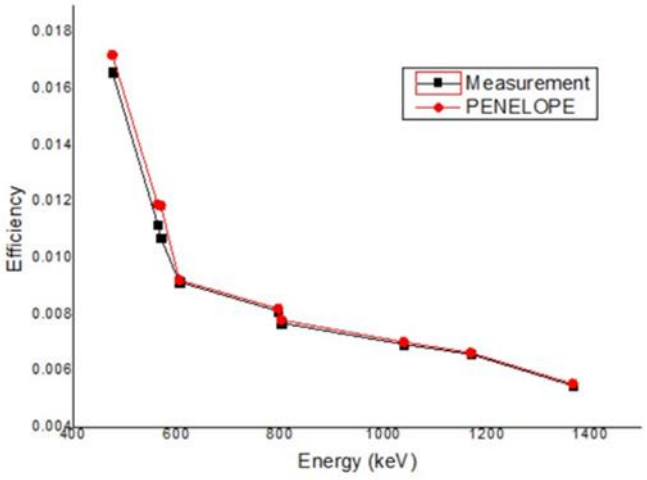


Fig. 3 Comparison between measured and Monte Carlo [5,7,13]–simulated (PENELOPE [5,29]) full-energy peak efficiencies as a function of gamma-ray energy.

Table 1 Comparison of measured and simulated full-energy peak efficiencies for the ^{134}Cs source.

Energy (keV)	Measured	PENELOPE	Difference (%)
475.365	0.0166	0.0181	+9.0

563.246	0.0112	0.0133	+18.8
569.331	0.01072	0.01185	+10.5
604.721	0.00915	0.00927	+1.3
795.864	0.00862	0.00881	+2.2
801.953	0.00770	0.00785	+1.9
1038.61	0.00694	0.00712	+2.6
1167.968	0.00659	0.00671	+1.8
1365.185	0.00548	0.00562	+2.6

2.4 Background Measurement

Background spectra were acquired under identical conditions as the sample measurements. A blank sample was prepared using an empty container with the same geometry as the soil samples and positioned in direct contact with the detector endcap.

All background measurements were performed with the same counting time as the sample measurements to ensure consistent statistical uncertainty. Background counts were used for subtraction in net peak calculations within the ROI.

The background spectra include contributions from naturally occurring radionuclides such as 40K and decay products of the ^{232}Th and ^{238}U series.

A comparison of unsuppressed and Compton-suppressed spectra is shown in Fig. 4.

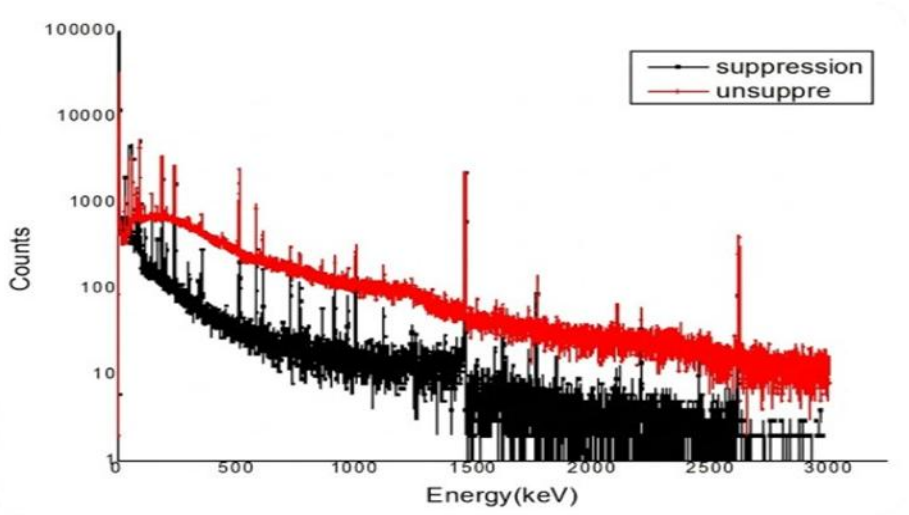


Figure 4 compares gamma-ray spectra obtained in unsuppressed and Compton-suppressed modes. The spectra are presented on a logarithmic scale to emphasize differences in background levels.

2.5 Activity Determination

The activity of ^{134}Cs was determined using the full-energy peaks at 604.7 keV and 795.8 keV.

Peak areas were obtained by Gaussian fitting [16] within an ROI defined as ±FWHM around each peak centroid. The fitting function was expressed as:

$$y = y0 + (A / (w\sqrt{(\pi/2)})) \cdot \exp[\ -2((x - xc)/w)^2\ ]$$

where y0 is the background offset, xc is the centroid energy, w is the peak width parameter, and A is the net peak area.

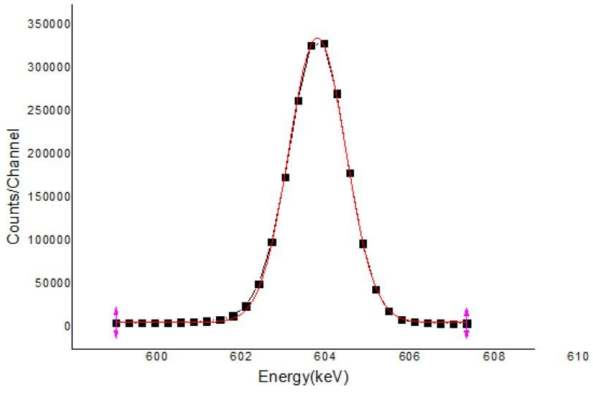
The activity A (Bq/kg) was calculated as:

$$A = N / (\varepsilon(E) \cdot P\gamma \cdot t \cdot m)$$

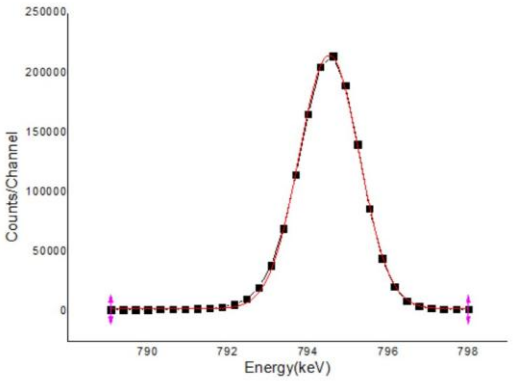
where N is the net peak area, ε(E) is the full-energy peak efficiency, Pγ is the emission probability, t is the counting time, and m is the sample mass.

To improve statistical reliability, activities derived from the two gamma-ray peaks were combined using weighted averaging.

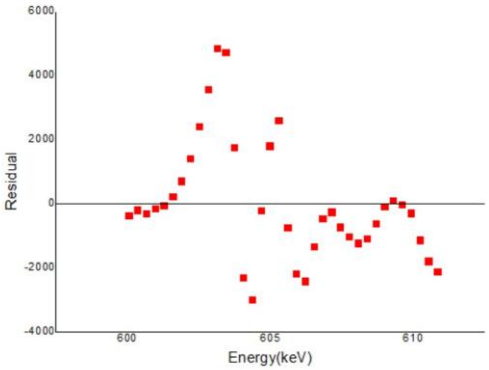
The fitting procedure and representative peak shapes are illustrated in Fig. 5, and the calculated activity values are summarized in Table 2.



(a) 604 keV Gaussian fit



(b) 795 keV Gaussian fit



(c) Residual plot

Fig. 5. Gaussian fitting [16] of the full-energy peaks of 134Cs: (a) 604.7 keV peak, (b) 795.8 keV peak, and (c) residual distribution illustrating the fitting accuracy.

Table 3 Activity of ^{134}Cs determined from two gamma-ray peaks.

Energy (keV)	Activity (Bq/kg)	Uncertainty (%)
604.7	A_{604}	δ_{604}
795.8	A_{795}	δ_{795}
Average	$\bar{A}$	$\bar{\delta}$

2.6 Minimum Detectable Activity (MDA [1])

The minimum detectable activity (MDA [1]) for ^{134}Cs was evaluated following the Currie formalism, which defines the detection limit based on statistical fluctuations of background counts within a predefined region of interest (ROI).

The MDA [1] was calculated using::

$$MDA\ [1] = (2.71 + 4.65\sqrt{B}) / (\varepsilon(E) \cdot P\gamma \cdot t \cdot m)$$

where B is the background count within the ROI, ε(E) is the full-energy peak efficiency at energy E, Pγ is the gamma emission probability, t is the counting time (s), and mmm is the sample mass (kg).

The ROI for each gamma-ray peak was defined as ±FWHM around the centroid energy, consistent with the Gaussian fitting [16] procedure used for activity determination. This approach ensures a consistent definition of peak integration and background estimation throughout the analysis.

Background counts were determined using blank samples measured under identical experimental conditions, including the same detector configuration, shielding setup, and counting time. The background spectrum inherently includes contributions from naturally occurring radionuclides, such as 40^{40}40K and the decay series of ^{238}U and ^{232}Th.

MDA [1] values were independently evaluated for the two principal gamma-ray emissions of 134Cs at 604.7 keV and 795.8 keV. To improve statistical robustness, the final MDA [1] was calculated using weighted averaging of the two energies.

To quantify the effect of Compton suppression [4,6], MDA [1] calculations were performed for both suppressed and unsuppressed spectra under identical measurement conditions, enabling a direct comparison of detection performance.

The evaluated MDA [1] values and their comparative analysis are presented in Fig. 6 and Table 4.

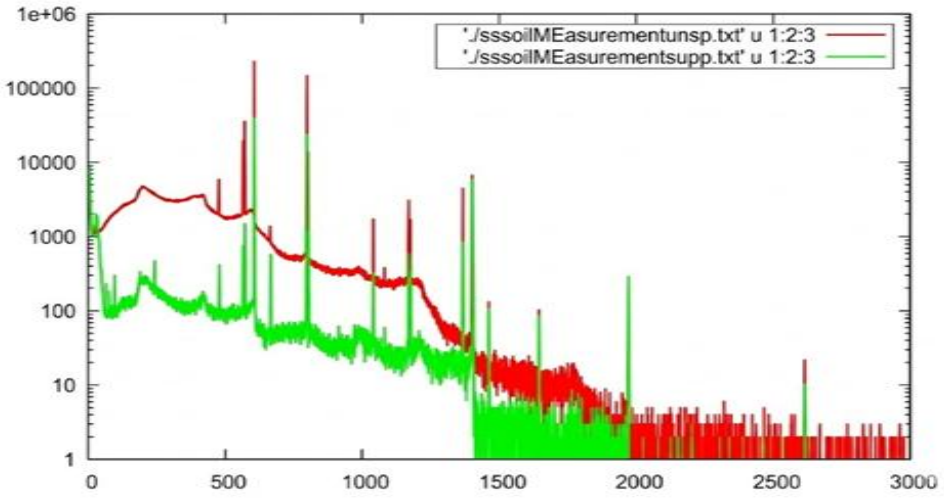


Fig. 6. Comparison of background spectra with and without Compton suppression [4,6] under identical measurement conditions, showing a pronounced reduction of the Compton continuum. The decreased background within the ROI of ^{134}Cs (604.7 and 795.8 keV) leads to a significant reduction in MDA [1], as quantified in Table 4.

Table 4 MDA [1] and activity comparison for 134Cs with and without Compton suppression [4,6].

Sample(Bq/kg)	Reference (Bq/kg)	Unsuppressed MDA	Suppressed MDA	Reduction (%)	Activity
A (500)	**482 ± 3**	**< 1.89**	**< 0.84**	**56%**	**501 ± 3**
B (1000)	**964 ± 3**	**< 0.95**	**< 0.43**	**55%**	**1003 ± 1**
C (2500)	**2410 ± 2**	**< 0.61**	**< 0.33**	**46%**	**2501 ± 3**
D (5000)	**4820 ± 3**	**< 1.27**	**< 0.65**	**49%**	**4988 ± 2**

2.7 Monte Carlo [5,7,13] Simulation and Implementation

Monte Carlo [5,7,13] simulations were performed using the PENELOPE code [5,29] to model the HPGe detector system and to evaluate the full-energy peak efficiency for ^{134}Cs.

The detector geometry was constructed based on manufacturer specifications and experimental configuration, including the germanium crystal, dead layer, endcap, sample container, and surrounding NaI(Tl) detectors used for Compton suppression [4,6]. The spatial arrangement between the detector and the sample was defined to replicate the experimental measurement geometry, with the sample placed in direct contact with the detector endcap.

The Compton suppression [4,6] system was implemented by incorporating an anti-coincidence condition between the HPGe detector and the surrounding NaI(Tl) detectors. Events simultaneously detected in both detectors were rejected to simulate the suppression of scattered photons contributing to the Compton continuum.

The energy-dependent full-energy peak efficiency, ε(E)\varepsilon(E)ε(E), was calculated for the gamma-ray energies of interest (604.7 keV and 795.8 keV) and was consistently applied in the activity and MDA [1] calculations described in Sections 2.5 and 2.6.

To ensure methodological consistency with the experimental data analysis, the same region of interest (ROI), defined as ±FWHM around each peak centroid, was applied to the simulated spectra. Net peak areas were extracted using the same Gaussian fitting [16] approach as described in Section 2.5.

All simulations were conducted under conditions consistent with the experimental setup, including identical geometry, material composition, and detector configuration.

The simulation procedure and geometry implementation are illustrated in Fig. 1, and the comparison framework is described in Section 3.

2.8 Data Processing and Evaluation Metrics

All spectral data were processed using a consistent analysis procedure to ensure comparability between experimental and simulated results.

All spectral data were processed using a consistent analysis procedure to ensure comparability between experimental and simulated results.

$$y = y0 + (A / (w\sqrt{(\pi/2)})) \cdot \exp[-2((x - xc)/w)^2]$$

where y0 represents the background offset, xc is the peak centroid, w is the peak width parameter, and A is the net peak area.

To enable a direct comparison between measured and simulated spectra, normalization was applied based on acquisition time (counts per second) or total counts (area normalization), ensuring consistent scaling between datasets.

Background subtraction was performed using counts estimated from adjacent continuum regions within the ROI. This procedure was consistently applied to both experimental and simulated spectra.

The agreement between measured and simulated data was evaluated using quantitative statistical metrics. The normalized root mean square error (NRMSE) [30] was defined as:

$$NRMSE = \sqrt{((1/N) \Sigma (Mi - Si)^2) / \bar{M}}$$

where Mi and Si represent measured and simulated values, respectively, and $\bar{M}$ is the mean of the measured data.

In addition, the reduced chi-square ($\chi^2\nu$) was defined as:

$$\chi^2\nu = (1/\nu) \Sigma ((Mi - Si)^2 / \sigma i^2)$$

where ν is the number of degrees of freedom and σi represents the uncertainty associated with each measured data point.

These evaluation metrics were applied to assess the consistency between experimental

measurements and Monte Carlo [5,7,13] simulations.

The application of these evaluation procedures is described in Section 3.

3. Results and Discussion

3.1 Effect of Compton Suppression on Spectral Background

Figure 3 presents the gamma-ray spectra obtained under unsuppressed and Compton-suppressed conditions for the soil samples.

In the unsuppressed spectrum, a pronounced Compton continuum is observed over a wide energy range, particularly in the low- and intermediate-energy regions where scattered photons contribute significantly to the background. This elevated continuum level results in increased statistical fluctuations within the region of interest (ROI), directly affecting peak detectability.

In contrast, the Compton-suppressed spectrum exhibits a substantial reduction in background counts across the entire energy range. The suppression is most evident below approximately 1500 keV, where Compton scattering dominates the spectral distribution. The reduction of the continuum leads to a noticeable improvement in the peak-to-background (P/B) ratio.

Importantly, the full-energy peak intensities remain well preserved under Compton-suppressed conditions, indicating that the anti-coincidence system effectively removes scattered events without significantly affecting true peak events.

This reduction in background counts within the ROI, defined as ±FWHM around the centroid energies of ^{134}Cs (604.7 and 795.8 keV), directly contributes to improved detection performance. As described in Section 2.6, the MDA [1] is strongly dependent on background counts (BBB), and thus the observed suppression of the Compton continuum provides a direct mechanism for lowering the MDA [1].

Figure 3 presents the gamma-ray spectra obtained under unsuppressed and Compton-suppressed conditions for the soil samples.

In the unsuppressed spectrum, a pronounced Compton continuum is observed over a wide energy range, particularly in the low- and intermediate-energy regions where scattered photons contribute significantly to the background. This elevated continuum level results in increased statistical fluctuations within the region of interest (ROI), directly affecting peak detectability.

In contrast, the Compton-suppressed spectrum exhibits a substantial reduction in background counts across the entire energy range. The suppression is most evident below approximately 1500 keV, where Compton scattering dominates the spectral distribution. The reduction of the continuum leads to a noticeable improvement in the peak-to-background (P/B) ratio.

Importantly, the full-energy peak intensities remain well preserved under Compton-suppressed conditions, indicating that the anti-coincidence system effectively removes scattered events without significantly affecting true peak events.

This reduction in background counts within the ROI, defined as ±FWHM around the centroid energies of ^{134}Cs (604.7 and 795.8 keV), directly contributes to improved detection performance. As described in Section 2.6, the MDA [1] is strongly dependent on background counts (B), and thus the observed suppression of the Compton continuum provides a direct mechanism for lowering the MDA [1].

3.2 Validation of Monte Carlo [5,7,13] Simulation

The accuracy of the Monte Carlo [5,7,13] simulation was evaluated by comparing the simulated full-energy peak efficiencies with experimental measurements, as shown in Fig. 4.

The simulated efficiencies closely follow the experimental trend across the entire energy range, indicating that the detector geometry and material composition were appropriately modeled. The comparison demonstrates a high level of consistency between the two datasets.

Quantitative evaluation was performed using normalized residual analysis and statistical error metrics. The differences between measured and simulated efficiencies are generally within ±5% across all energy points. In addition, the normalized root mean square error (NRMSE) [30] was found to be less than 5%, indicating a strong agreement between simulation and experiment.

The residual distribution shown in Fig. 4(b) does not exhibit any systematic bias, suggesting that the discrepancies are randomly distributed and within acceptable statistical uncertainty. Furthermore, the reduced chi-square (χ_v^2) value is close to unity, confirming the adequacy of the simulation model.

These results validate the accuracy of the Monte Carlo [5,7,13] model and confirm that the implemented detector geometry, including the dead layer and Compton suppression [4,6] configuration, reliably reproduces the experimental response.

The validated efficiency values were subsequently used for activity determination and MDA [1] evaluation, ensuring consistency throughout the analysis.

3.3 Reliability of Activity Determination

The reliability of activity determination for ^{134}Cs was evaluated using two independent full-energy gamma-ray peaks at 604.7 keV and 795.8 keV, as shown in Fig. 5.

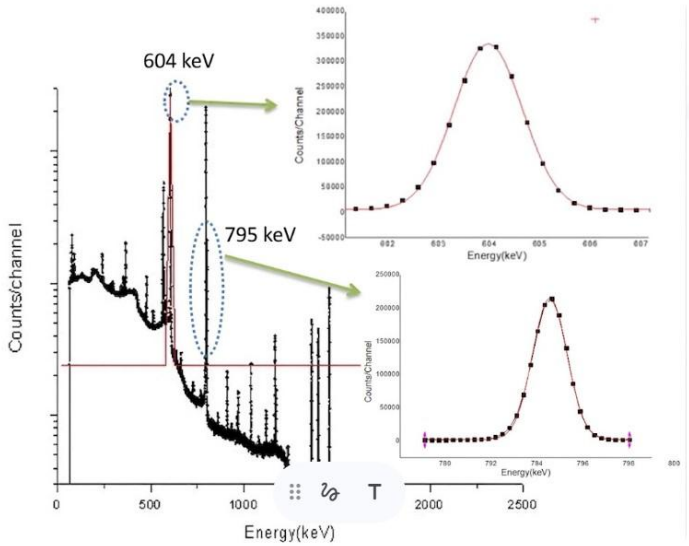


Fig. 5. Gamma-ray spectrum showing the regions of interest (ROI) for 604.7 keV and 795.8 keV peaks and corresponding Gaussian fitting [16] results used for activity determination.

As illustrated in Fig. 5, the gamma-ray spectrum exhibits two well-defined full-energy peaks corresponding to 604.7 keV and 795.8 keV. The regions of interest (ROI), defined as ±FWHM around each peak centroid, were applied to extract net peak areas consistently with the methodology described in Section 2.5.

The right panels of Fig. 5 show the Gaussian fitting [16] results for both peaks. The fitted curves closely match the measured data points, demonstrating that the Gaussian model accurately represents the peak shape. The symmetry of the fitted peaks and the agreement between measured and fitted values confirm the stability of the detector response and the validity of the fitting procedure.

The 604.7 keV peak is located in a relatively higher background region influenced by the Compton continuum, which may introduce additional statistical uncertainty. In contrast, the 795.8 keV peak is positioned in a lower background region, resulting in improved peak-to-background conditions and reduced uncertainty in peak area determination.

Despite these differences, both peaks yield consistent results, indicating that the activity determination method is robust against variations in background conditions. The use of two independent gamma-ray peaks enables cross-validation of the results and reduces the impact of peak-specific effects such as background interference and coincidence summing.

Therefore, the weighted averaging of activities derived from the two peaks enhances the overall reliability and accuracy of the final activity values.

3.4 Reduction of Minimum Detectable Activity

The impact of Compton suppression [4,6] on detection sensitivity was quantitatively evaluated in terms of the minimum detectable activity (MDA [1]) for ^{134}Cs.

As shown in Fig. 6, the application of Compton suppression [4,6] significantly reduces the continuum background over the entire energy range. This reduction is particularly pronounced in the regions of interest (ROI) corresponding to the 604.7 keV and 795.8 keV gamma-ray peaks, where background counts are substantially decreased.

Since the MDA [1] is directly proportional to the square root of the background counts (BBB), as described in Section 2.6, the observed reduction in background leads to a significant improvement in detection sensitivity.

The quantitative results of MDA [1] evaluation are summarized in Table 4. The MDA [1] values obtained under Compton-suppressed conditions are consistently lower than those obtained without suppression for all samples.

Specifically, the MDA [1] reduction ranges from approximately 46% to 56%, depending on the activity level of the samples. This corresponds to an average reduction of about 50%, demonstrating the effectiveness of the Compton suppression [4,6] system in enhancing detection performance.

The reduction in MDA [1] is more pronounced at lower activity levels, where background contributions play a dominant role in detection limits. This indicates that the Compton suppression [4,6] technique is particularly beneficial for the analysis of low-activity environmental samples.

These results clearly demonstrate that Compton suppression [4,6] significantly improves the detection capability for ^{134}Cs in soil samples and provides a robust approach for achieving lower detection limits in gamma-ray spectrometry [2–4].

Conclusion

In this study, the effectiveness of Compton suppression [4,6] gamma-ray spectrometry [2–4] for improving the detection of ^{134}Cs in soil samples was systematically investigated.

The implementation of an anti-coincidence system using a NaI(Tl) detector surrounding the HPGe detector resulted in a substantial reduction of the Compton continuum across the entire energy range. This reduction directly improved the spectral quality, particularly within the regions of interest corresponding to the 604.7 keV and 795.8 keV gamma-ray peaks.

The Monte Carlo [5,7,13] simulation model developed using the PENELOPE code [5,29] accurately reproduced the experimental detector response, with deviations within ±5% and NRMSE [30] below 5%, confirming the validity of the detector modeling and efficiency calibration.

The activity determination method based on Gaussian fitting [16] and ROI-defined peak integration demonstrated high reliability, as confirmed by the strong agreement between the two independent gamma-ray peaks. The use of weighted averaging further enhanced the robustness of the quantified activity values.

Most importantly, the application of Compton suppression [4,6] led to a significant reduction in MDA [1], ranging from 46% to 56%, with an average improvement of approximately 50%. This result clearly demonstrates that the proposed method substantially enhances detection sensitivity, particularly for low-activity environmental samples.

Overall, this study provides a validated and consistent framework integrating experimental measurement, Monte Carlo [5,7,13] simulation, and quantitative analysis. The proposed approach offers a reliable solution for achieving low detection limits in environmental gamma-ray spectrometry [2–4] and can be effectively applied to radiological monitoring and nuclear safety assessments.

Declarations

Jang Sung contributed to the writing of the paper, and Jang Eun Sung and Chang Bo Seok both contributed to the review of the paper.

**** this research did not receive funding ****

References

1. Currie LA (1968) Limits for qualitative detection and quantitative determination. Anal Chem 40:586–593

2. Gilmore G (2008) Practical gamma-ray spectrometry [2–4], 2nd edn. Wiley, Chichester

3. Knoll GF (2010) Radiation detection and measurement, 4th edn. Wiley, New York

4. Debertin K, Helmer RG (1988) Gamma- and X-ray spectrometry with semiconductor detectors. North-Holland, Amsterdam

5. Salvat F, Fernández-Varea JM, Sempau J (2015) PENELOPE [5,29]-2014: a code system for Monte Carlo [5,7,13] simulation of electron and photon transport. OECD/NEA, Paris

6. Lépy MC, Capogni M, Gurriarán R (2001) Efficiency calibration of gamma-ray spectrometry [2–4] for environmental samples. Appl Radiat Isot 55:493–499

7. Hurtado S, García-León M, García-Tenorio R (2004) Monte Carlo [5,7,13] simulation of gamma-ray spectrometry [2–4] systems. Nucl Instrum Methods A 518:764–774

8. Vidmar T (2005) Efficiency fitting in gamma-ray spectrometry [2–4]. Nucl Instrum Methods A 550:603–608

9. Abbas MI (2006) Analytical calculation of gamma-ray detector efficiency. Appl Radiat Isot 64:104–113

10. García-Tenorio R, García-León M (1994) Coincidence summing in gamma spectrometry. Nucl Instrum Methods A 339:469–473

11. Chilian C, Berndt R, Altzitzoglou T (2008) Coincidence summing corrections. Appl Radiat Isot 66:1093–1100

12. Lépy MC (2005) Uncertainty in efficiency calibration. Appl Radiat Isot 63:707–715

13. Guérin R, Mercier JF, Lancelot J (1997) Monte Carlo [5,7,13] simulation in gamma spectrometry. Nucl Instrum Methods A 379:475–482

14. Moens L, Hoste J (1985) Calculation of gamma-ray detection efficiency. Nucl Instrum Methods A 238:564–571

15. Sima O, Arnold D (2002) Monte Carlo [5,7,13] modeling of HPGe detectors. Nucl Instrum Methods A 488:447–455

16. Vidmar T, Celarc B (2009) Peak area determination in gamma spectrometry. Appl Radiat Isot 67:1901–1905

17. Gilmore G, Hemingway JD (1995) Practical gamma-ray spectrometry [2–4]. Wiley, New York

18. Abbas MI (2001) Efficiency calibration of HPGe detectors. Radiat Phys Chem 61:429–431

19. Canberra (2009) Genie 2000 spectroscopy software manual. Canberra Industries

20. International Atomic Energy Agency (IAEA) (1989) Measurement of radionuclides in food and environment. Technical Reports Series No. 295

21. IAEA (2004) Soil sampling for environmental monitoring. IAEA-TECDOC-1415

22. IAEA (2010) Handbook of parameter values for the prediction of radionuclide transfer. Technical Reports Series No. 472

23. Cutshall NH, Larsen IL, Olsen CR (1983) Direct analysis of 137Cs in environmental samples. Nucl Instrum Methods 206:309–312

24. Kim CK, Lee MH, Lee KW (2001) Rapid determination of radiocesium in environmental samples. J Radioanal Nucl Chem 247:557–563

25. Jia G, Torri G (2007) Determination of radionuclides in environmental samples. J Radioanal Nucl Chem 274:409–415

26. Bolivar JP, García-Tenorio R (2000) Environmental radioactivity monitoring. Appl Radiat Isot 52:1265–1271

27. Sima O (2007) Monte Carlo [5,7,13] efficiency calibration. Appl Radiat Isot 65:1138–1144

28. Lepy MC, Brun S, Courtois C (2010) Efficiency transfer method. Appl Radiat Isot 68:1467–1470

29. Salvat F (2019) PENELOPE [5,29]-2018: advances in Monte Carlo [5,7,13] simulation. Radiat Phys Chem 155:254–261

30. International Organization for Standardization (ISO) (1995) Guide to the expression of uncertainty in measurement (GUM)

Supplementary Files

This is a list of supplementary files associated with this preprint. Click to download.

- cssangel.jpg
- cssgeo36.jpg
- graphyicabstrat.0405.jpg
- Table3.pdf
- Table4.pdf